IEEE Access
Multidisciplinary | Rapid Review | Open Access Journal

Received December 4, 2019, accepted December 9, 2019, date of publication December 13, 2019,
date of current version December 23, 2019.

Digital Object Identifier 10.1109/ACCESS.2019.2959296

Modeling and Position Tracking Control of a Novel Circular Hydraulic Actuator With Uncertain Parameters

MINGXING YANG, KAIWEI MA, YUNDE SHI, AND XINGSONG WANG
School of Mechanical Engineering, Southeast University, Nanjing 211189, China

Corresponding author: Xingsong Wang (xswang@seu.edu.cn)

This work was supported in part by the National Natural Science Foundation of China under Grant 51575100 and Grant 61903186, in part by the Natural Science Foundation of Jiangsu Province, China, under Grant BK20190665, and in part by the Postgraduate Research and Practice Innovation Program of Jiangsu Province under Grant KYCX18_0065.

ABSTRACT In order to realize precise position tracking of a novel circular hydraulic actuator with parameter uncertainties and bounded disturbances, an adaptive sliding mode controller (ASMC) that incorporates a fuzzy tuning technique is proposed in this paper. The mechanical structure and basic principle of the actuator are first introduced, and the mathematical model of its corresponding valve-controlled hydraulic servo system is constructed. Based on Lyapunov stability theory, online parameter estimation and sliding mode controller design are effectively integrated to approximate the equivalent control of sliding mode. To mitigate the undesired chattering phenomenon and further improve system performance, a fuzzy tuning scheme is employed to regulate the proportional gain of the approaching control term. In addition, a real-time control platform is established, and the controllers parameter identification and position tracking are verified by preliminary experiments. Finally, the traditional PID controller and the exponent approaching sliding controller are also conduced to further evaluate the control performances of the designed controller, and the comparative results demonstrate that the proposed control scheme has better control performance in reducing errors for trajectory tracking.

INDEX TERMS Position tracking, circular hydraulic actuator, parameter uncertainties, adaptive sliding mode control, fuzzy tuning scheme.

I. INTRODUCTION

The electro-hydraulic servo system (EHSS) possesses excellent practical features and high reliability in industrial automation fields for its merits of small size-to-power ratio, large force output capability and fast response. However, it is a nonlinear system with serious uncertainties due to existing friction, leakages and variable oil temperature [1]–[4]. Apart from high nonlinearity and parameter uncertainties, the un-modeled dynamics caused by the high frequency response of servo valve and external load is another problem that can not be ignored in hydraulic system control [5]. As a consequence, precise motion control of hydraulic systems is a challenging task for both academia and engineering [6]–[8]. In the past several years, tracking control of nonlinear electro-hydraulic systems with uncertain parameters or unknown dynamics has attracted great attention.

PID and linear controllers are common control methods for EHSS due to their simplicity and easy to operate [9], but the performance is usually poor when applied to models with time-varying parameters and external disturbances. By contrast, sliding mode control (SMC) features excellent robustness properties in relation to parametric uncertainties [10]–[13], which has been applied by many researchers to the position control of hydraulic systems. In [14], [15], a sliding mode adaptive controller was proposed to deal with nonlinear uncertain parameters caused by variations of the original control volumes or pressures. Two different sliding mode observers were presented in [16] to estimate the uncertain disturbances caused by friction acting on the hydraulic cylinder and the dead-zone in the valve. Also, the authors in [17] combined sliding mode controller with an adaptive backstepping technique to drive a

The associate editor coordinating the review of this manuscript and approving it for publication was Zhuang Xu.

hydraulic manipulator with actuator dynamics. Moreover, both fuzzy control and neural networks are ideal strategies to approximate the uncertain nonlinear dynamical system. In [18]–[20], sliding-mode control incorporated with a fuzzy tuning technique was employed in hydraulic systems to deal with parameter uncertainties and external disturbances. In order to realize precise motion control of the hydraulic servo system with mismatched uncertainties, [21], [22] combined the neural networks technique with the sliding mode control to learn the behavior of the uncertain nonlinear functions. While these advanced nonlinear control techniques demonstrate excellent robustness to parametric uncertainties and external disturbances, pressure and position sensors have to be installed accurately for state measurement in most cases [10], [23], [24]. Besides, intelligent control methods increase the complexity of control algorithm and time consumption so they are rarely adopted to estimate uncertain parameters in practical applications.

As is well known, SMC relies on a discontinuous control action to force the trajectory to reach a desired sliding surface in finite time and then stay on it for all future time [5], [25]. In other words, the SMC can effectively keep the hydraulic position servo system stable when the switching gain of discontinuous control is properly selected. However, due to the strong nonlinearity and parameter uncertainty of the hydraulic system, the inherent chattering caused by discontinuous control action of SMC can easily excite high frequency dynamics and degrade system performance [26]–[28]. Therefore, to obtain better dynamic performance, considerable attention has been paid to eliminate the chattering problem in control of such mechanisms. In [29], [30], a sliding mode control with varying boundary layers was used to decrease the chattering phenomenon for position tracking of a nonlinear electro-hydraulic position servo system. It was confirmed in [31]–[33] that exponential reaching law was an effective method to decrease chattering of the sliding mode control, however, the large gain coefficients will degrade the performance of hydraulic systems. To improve the dynamic performance and eliminate the high-frequency chattering, a weighting factor estimation technique was introduced in [34]. Besides, [35] combined a direct adaptive fuzzy scheme and a fuzzy sliding scheme to reduce the tracking error and the chattering of the hydraulic system. In order to eliminate the chattering in SMC, [36] introduced a fuzzy self-turning mechanism to regulate two gain coefficients of the exponential reaching law according to several conditions. Nevertheless, this control method may be restricted in practical applications as it requires significant computation power and expert experience.

In summary, compared with other advanced nonlinear control techniques, ASMC has the advantages of easy implementation, strong adaptability and insensitive to parameter variations, and which is the preferred option for nonlinear hydraulic system. Moreover, the combination of exponential reaching law and fuzzy self-tuning mechanism can effectively reduce the chattering phenomenon caused by discontinuous switches control of SMC. Thus, utilizing the advantages of adaptive control and fuzzy logical, a novel adaptive fuzzy sliding mode controller (AFSMC) is presented to realize continuous on-line trajectory tracking of the circular electro-hydraulic actuator. Main contributions of this paper are listed as follows: (1) A novel circular hydraulic actuator is designed that can be directly and compactly installed at the hip joint. The angular displacement of the piston rod is synchronous with the swing of the joint rod which solves the problem of transmission nonlinearity caused by the installation geometry of the linear hydraulic rod at the joint. (2) The fuzzy control method is incorporated into the exponential reaching law to solve the chattering problem caused by the discontinuous switching action. Compared to other direct adaptive controllers [34], [35], this scheme of adjusting the proportional gain by using fuzzy control under the premise of ensuring the stability of the system is simple and transparent. It not only solves the complex control problem in practical applications but also improves the system performance.

The remainder of this paper is organized as follows. The circular electro-hydraulic actuator is detail introduced and its corresponding mathematical modeling is derived in Section II. In Section III, the adaptive sliding mode controller with fuzzy self-tuning mechanism is discussed. Then, the experimental evaluation of the proposed controller is discussed in Section IV and the comparison to the other two controllers are presented to show the effectiveness and superiority of the proposed method. Finally, conclusions and future works are drawn in Section V.

II. STRUCTURAL DESIGN AND SYSTEM DYNAMIC MODELING

The circular hydraulic actuator discussed in this paper is installed on the hip exoskeleton, which is used primarily to provide power assistance for human walking. The gait analysis and biomechanical characteristics of human hip joint are studied in [37]. Then, the structural design of the circular hydraulic actuator and the dynamic model of the valve-controlled hydraulic servo system are presented below.

A. STRUCTURAL DESIGN OF THE CIRCULAR HYDRAULIC ACTUATOR

The construction of the circular hydraulic actuator is depicted in Fig. 1. Its major components include a hydraulic cylinder block, a curved piston rod integrated with piston, a fixed shaft, two bearings, an angular sensor, a guide sleeve, two rigid links, some screws and dowel pins. Moreover, some sealing components are indispensable parts in hydraulic design to prevent internal oil leakage between two chambers and external oil leakage from the chamber to the environment. For simplicity, the cylinder block is made of two approximately symmetrical cylinder heads, which are aligned by the dowel pins and tightened by the screws with elastic washers. The piston rod has sealing rings installed on one end and is fixed to the rigid links by two screws on the other end.

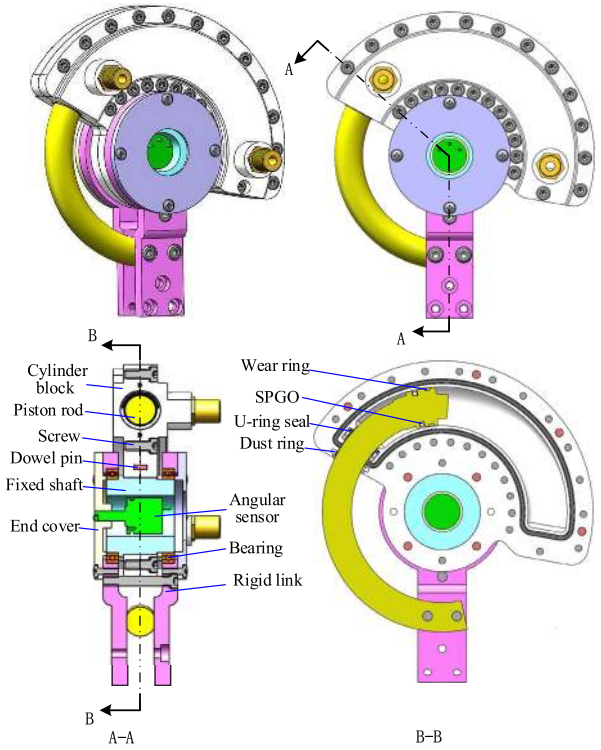

FIGURE 1. Structure models of the circular hydraulic actuator.

The basic working principle of the circular hydraulic actuator is similar to the linear hydraulic rod. The servo valve regulates the oil flow into rod chamber and rodless chamber of the circular hydraulic cylinder, thereby generating a pressure difference between the two chambers of the hydraulic cylinder to drive the connecting rod. As a result, the piston rod moves in the circular chamber of the cylinder block under the action of high oil pressure, which drives the rigid links to rotate around the fixed shaft. Obviously, the circular cylinder actuator can be designed to the required size according to the actual requirements, and can be directly and compactly installed at the hip joint. Moreover, the angular displacement of the piston rod is synchronous with the swing of the joint rod, which solves the problem of transmission nonlinearity caused by the installation geometry of the linear hydraulic rod at the joint.

B. DYNAMIC MODES OF THE HYDRAULIC SERVO SYSTEM

Structure diagram of the electro-hydraulic position servo system discussed in this paper is depicted in Fig. 2. It mainly consists of a circular hydraulic actuator, an angle sensor, a four-way spool valve, and a hydraulic workstation with other components.

Assuming that the supply pressure P_s is constant and its return line pressure P_t is zero. Thus, the flow rates Q_1 and Q_2 of the servo valve can be calculated as [14]

$$\begin{aligned} Q_1 &= C_d x_v w \sqrt{\left[P_s + sgn(x_v)(P_s - 2P_1)\right]/\rho} \\ Q_2 &= C_d x_v w \sqrt{\left[P_s + sgn(x_v)(2P_2 - P_s)\right]/\rho} \end{aligned} \tag{1}$$

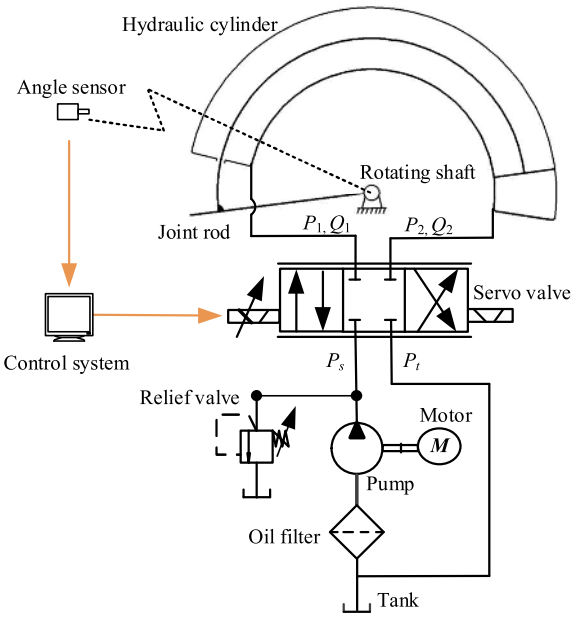

FIGURE 2. Structure diagram of electro-hydraulic position servo control system.

where C_d is the flow modification coefficient, x_v is the servo valve spool displacement, w is the valve area gradient, p_1 and p_2 are the pressures inside two chambers of the cylinder, and ρ is the oil density.

Considering that the leakage flow is as insignificant as the fluid compression, the following approximation is obtained

$$Q_2/Q_1 \approx A_2/A_1 = \varepsilon \tag{2}$$

where ε denotes the piston area ratio.

Furthermore, define the load pressure P_l and the load flow Q_l of the system as

$$\begin{aligned} P_l &= P_1 - \varepsilon P_2 \\ Q_l &= (Q_1 + \varepsilon Q_2) \Big/ \left(1 + \varepsilon^2\right) = Q_1 \end{aligned} \tag{3}$$

Assuming zero opening of sliding valve at the starting point of the piston rod, by Taylor expansion, the load flow equation can be linearized as [38]

$$Q_l = K_q x_v - K_c P_l \tag{4}$$

where K_q and K_c are the flow-gain coefficient and the flow-pressure coefficient of the servo valve, respectively, which can be described by

$$\begin{aligned} K_q &= C_d w \sqrt{\frac{(1+\varepsilon) P_s + sgn(x_v)\left[(1-\varepsilon) P_s - 2P_l\right]}{\rho(1+\varepsilon^3)}} \\ K_c &= \frac{C_d w x_v}{\sqrt{\rho(1+\varepsilon^3)\left\{(1+\varepsilon) P_s + sgn(x_v)\left[(1-\varepsilon) P_s - 2P_l\right]\right\}}} \end{aligned}$$

By neglecting the elasticity of the compressible fluid, the flow continuity equations of two chambers can be given

as [5], [39]

$$Q_1 = C_i(P_1 - P_2) + C_e P_1 + A_1 R\dot{\theta}_p + \frac{V_{10}+A_1 R\theta_p}{\beta_e}\dot{P}_1$$
$$Q_2 = C_i(P_1 - P_2) - C_e P_2 + A_2 R\dot{\theta}_p + \frac{V_{20}-A_2 R\theta_p}{\beta_e}\dot{P}_2 \quad (5)$$

where V_{10} and V_{20} are the original total volumes of the fluid between the valve and two actuator chambers respectively, β_e represents the effective hydraulic fluid bulk modulus, C_i and C_e denote the coefficients of the internal leakage and the external leakage of the cylinder, respectively, and θ_p is the angular displacement of the rod.

Combing (3) with (5), the load pressure Q_l is rewritten as

$$Q_l = A_1 R\dot{\theta}_p + \lambda_1\dot{P}_l + \lambda_2 P_l + \lambda_3 P_s \quad (6)$$

where

$$\lambda_1 = \frac{V_{10}V_{20}}{\beta_e\left(\varepsilon^2 V_{10} + V_{20}\right)}$$
$$\lambda_2 = \frac{\left(\varepsilon^3 V_{10} + V_{20}\right)(C_i + C_e) + \varepsilon\left(V_{10} + \varepsilon V_{20}\right)C_i}{\left(1+\varepsilon^3\right)\left(\varepsilon^2 V_{10} + V_{20}\right)}$$
$$\lambda_3 = \frac{\varepsilon\left(V_{20} - V_{10}\right)(C_i + C_e) - \left(V_{20} - \varepsilon^2 V_{10}\right)C_i}{\left(1+\varepsilon^3\right)\left(\varepsilon^2 V_{10} + V_{20}\right)}\varepsilon^{1+sgn(u)}$$

In addition, with the combined action of internal hydraulic pressure and external disturbance moments, the equation of dynamic equilibrium can be established as

$$(P_1A_1 - P_2A_2)R = T_l + B_t R^2\dot{\theta}_p + J_l\ddot{\theta}_p \quad (7)$$

where A_1 and A_2 denote the effective ram areas of the two chambers, R is the curvature radius of the piston rod, T_l is the external disturbance torque, B_t represents the viscous damping coefficient, and J_l is the inertia moment of the piston rod and payload.

Since the natural frequency of the servo valve is much higher than that of the circular hydraulic cylinder, the relationship between spool displacement and input voltage can be expressed as [5]

$$x_v = K_v u \quad (8)$$

where K_v is the servo amplifier gain, and u is the control input voltage.

For simplicity, it is supposed that deformation of tubing from the servo valve to the two chambers can be neglected and the oil leakage is also insignificant. As mentioned above, choosing the system state variables as $[x_1, x_2, x_3]^T = [\theta_p, \dot{\theta}_p, \ddot{\theta}_p]^T$, the state equations of the valve-controlled hydraulic actuator system can be expressed as

$$\begin{aligned}\dot{x}_1 &= x_2\\ \dot{x}_2 &= x_3\\ \phi_1\dot{x}_3 &= -\phi_2 x_2 - \phi_3 x_3 + u - d_t\end{aligned} \quad (9)$$

where

$$\phi_1 = \frac{V_{10}V_{20}J_l}{K_q K_v\beta_e A_1 R\left(\varepsilon^2 V_{10} + V_{20}\right)}$$
$$\phi_2 = \frac{A_1^2 R^2 + K_c B_t R^2}{K_q K_v A_1 R}$$
$$\phi_3 = \frac{K_c\beta_e J_l\left(\varepsilon^2 V_{10} + V_{20}\right) + V_{10}V_{20}B_t R^2}{K_q K_v\beta_e A_1 R\left(\varepsilon^2 V_{10} + V_{20}\right)}$$
$$d_t = \frac{\beta_e K_c T_l\left(\varepsilon^2 V_{10} + V_{20}\right) + \dot{T}_l V_{10}V_{20}}{K_q K_v\beta_e A_1 R\left(\varepsilon^2 V_{10} + V_{20}\right)}$$

III. CONTROLLER DESIGN

The control task of this section is to find an appropriate controller such that the rod can track the desired trajectories as closely as possible. Based on this, the following assumptions should be considered.

Assumption 1: For the desired trajectory x_d, its first derivative $\dot{x}_d$, second derivative $\ddot{x}_d$ and third derivative $\dddot{x}_d$ with respect to time are all bounded.

Assumption 2: The generalized parameters ϕ_1, ϕ_2 and ϕ_3 are unknown and positive, but they can be confined in certain ranges, i.e., $\phi_{i\min} \le \phi_i \le \phi_{i\max}$, where $\phi_{i\min}$ and $\phi_{i\max}$ $(i = 1, 2, 3)$ are given positive constants. Moreover, the generalized external disturbance d_t has an upper bound D with $|d_t| \le D$.

A. SLIDING MODEL CONTROL WITH PARAMETRIC ADAPTIVE SCHEME

The defined command signal of electro-hydraulic position servo control system is θ_d, and the corresponding tracking error is $e = \theta_d - x_1$. By applying a stable filter and differential to x_1, we can get x_2 and x_3, respectively. On this basis, the corresponding derivatives $e_2 = \dot{\theta}_d - x_2$ and $e_3 = \ddot{\theta}_d - x_3$ are also easy to be calculated. Thus, the tracking error vector of the system can be described as

$$[e_1, e_2, e_3]^T = [e, \dot{e}, \ddot{e}]^T = \left[\theta_d - x_1, \dot{\theta}_d - x_2, \ddot{\theta}_d - x_3\right]^T \quad (10)$$

Then, a time-varying dynamic sliding surface s in the error state space is given by

$$s(t) = c_1 e_1 + c_2 e_2 + e_3 \quad (11)$$

where c_1 and c_2 are strictly positive constants that can be calculated in accordance with the pole collocation method or specified by the desired dynamics of the closed-loop system. Based on this, the tracking problem can be regarded as the state error vector reaching the desired sliding surface $s(t) = 0$ in finite time and then staying on it for the time left.

According to (9)-(11), the time derivative of s can be described as

$$\begin{aligned}\phi_1\dot{s}(t) &= \phi_1\left(c_1 e_2 + c_2 e_3 + \dot{e}_3\right)\\ &= \phi_1\left(c_1 e_2 + c_2 e_3 + \dddot{\theta}_d\right) + \phi_2 x_2 + \phi_3 x_3 - u + d_t\end{aligned} \quad (12)$$

Since $\phi_i (i = 1, 2, 3)$ are unknown time-varying parameters, an adaptive algorithm is introduced to estimate the unknown parameters of the system. It is assumed that the uncertain parameter $\phi_i (i = 1, 2, 3)$ is estimated by $\hat{\phi}_i$, i.e.

$$\tilde{\phi}_i = \phi_i - \hat{\phi}_i \quad (13)$$

where $\tilde{\phi}_i$ represents the ideal estimation error of ϕ_i. In addition, assuming these unknown parameters change slowly, i.e. $\dot{\phi}_1 \approx \dot{\phi}_2 \approx \dot{\phi}_3 \approx 0$, then $\dot{\tilde{\phi}}_i = -\dot{\hat{\phi}}_i$.

Taking into account (12) and (13), the equivalent control term can be given as follows

$$\hat{u}_{eq} = \hat{\phi}_1 \left(c_1 e_2 + c_2 e_3 + \dddot{\theta}_d\right) + \hat{\phi}_2 x_2 + \hat{\phi}_3 x_3 \tag{14}$$

Nevertheless, the system generally behaves as $s(t) \neq 0$ at the beginning or when system structure changes. Thus, an approaching control term u_{ap} based on the exponential approaching law will be added as

$$u_{ap} = k_s s + \eta_s sgn\,(s) \tag{15}$$

where $k_s > 0$ represents the proportional gain, and $\eta_s > D$ denotes the switching gain.

Therefore, the complete ASMC algorithm can be written as

$$\begin{aligned} u &= \hat{u}_{eq} + u_{ap} \\ &= \hat{\phi}_1 \left(c_1\, e_2 + c_2\, e_3 + \dddot{\theta}_d\right) + \hat{\phi}_2\, x_2 + \hat{\phi}_3\, x_3 + k_s s + \eta_s sgn\,(s) \end{aligned} \tag{16}$$

Here, u_{eq} determines the dynamics of the system on the sliding surface, and u_{ap} can eliminate the influence of perturbations and ensure the system states lying on the sliding surface.

Proof: The Lyapunov candidate function is defined as

$$V = \frac{1}{2}\phi_1 s^2 + \sum_{i=1}^{3} \frac{1}{2\gamma_i} \tilde{\phi}_i^2 \tag{17}$$

According to (13) and (16), the time derivation of the above equation can be obtained by

$$\begin{aligned} \dot{V} &= \phi_1\, s\dot{s} + \sum_{i=1}^{3} \frac{1}{\gamma_i} \tilde{\phi}_i \dot{\tilde{\phi}}_i \\ &= s\tilde{\phi}_1 \left(c_1\, e_2 + c_2\, e_3 + \dddot{\theta}_d\right) + \sum_{i=2}^{3} s\tilde{\phi}_i x_i \\ &\quad + s\left[-k_s s - \eta_s sgn\,(s) + d_t\right] - \sum_{i=1}^{3} \frac{1}{\gamma_i} \tilde{\phi}_i \dot{\hat{\phi}}_i \\ &= \tilde{\phi}_1 \left[\left(c_1\, e_2 + c_2\, e_3 + \dddot{\theta}_d\right) s - \frac{1}{\gamma_1} \dot{\hat{\phi}}_1\right] \\ &\quad + \sum_{i=2}^{3} \tilde{\phi}_i \left(s x_i - \frac{1}{\gamma_i} \dot{\hat{\phi}}_i\right) + s\left[-k_s s - \eta_s sgn\,(s) + d_t\right] \end{aligned} \tag{18}$$

Besides, the following adaptation law will be chosen to update the above tunable parameters

$$\begin{aligned} \dot{\hat{\phi}}_1 &= \gamma_1 s \left(\dddot{\theta}_d + c_1 e_2 + c_2 e_3\right) \\ \dot{\hat{\phi}}_2 &= \gamma_2 s x_2 \\ \dot{\hat{\phi}}_3 &= \gamma_3 s x_3 \end{aligned} \tag{19}$$

where γ_i $(i = 1, 2, 3)$ are strict positive constants to ensure the best possible estimates $\hat{\phi}_i$.

Substituting the above adaptation law into (18), the following equation can be obtained

$$\dot{V} = -k_s s^2 - \eta_s |s| + d_t s \leq -k_s s^2 - (\eta_s - D)|s| \tag{20}$$

Obviously, $\dot{V} \leq 0$ is guaranteed as long as $\eta_s > D$ and $k_s > 0$, and the function in (17) is positive definite. Besides, $s(t)$ goes to zero as t approaches infinity, which implies that the trajectory tracking error will asymptotically converge to zero. Therefore, according to the system input (16) and adaptation laws (19), the stability of the target system (9) is guaranteed.

Remark 1: In the initial stage, there may be a large gap between the actual position signal and the target signal of the system. Then, the adaptation law will force the corresponding parameters to change significantly to cope with the current state of the system. In addition, in the process of output tracking, the error fluctuation caused by external interference will also cause great changes to parameter identification. However, the excessive estimation of parameters may seriously affect the stability of the controller or even destroy the system.

In general, the discontinuous projection mapping [18] is a direct and effective method to deal with the overestimation of parameters. Hence, the parametric adaptive law (19) will be restricted as

$$Proj_{\hat{\phi}_i}(\lambda_i \psi_i) = \begin{cases} 0, & if\ \ \hat{\phi}_i = \phi_{i\max}\ and\ \lambda_i \psi_i > 0 \\ 0, & if\ \ \hat{\phi}_i = \phi_{i\min}\ and\ \lambda_i \psi_i < 0 \\ \lambda_i \psi_i, & otherwise \end{cases} \tag{21}$$

where $\psi_1 = s\left(\dddot{\theta}_d + c_1\, e_1 + c_2\, e_2\right)$, $\psi_2 = s x_2$ and $\psi_3 = s x_3$. Besides, the inequality $\phi_{i\min} \leq \hat{\phi}_i(t) \leq \phi_{i\max}$ is satisfied [9] as long as the initial value of $\hat{\phi}_i(0)$ is described as $\phi_{i\min} \leq \hat{\phi}_i(0) \leq \phi_{i\max}$.

B. FUZZY SELF-TUNING MECHANISM FOR THE PROPORTIONAL GAIN

As for adaptive sliding mode control (ASMC), precise estimation of adaptive strategy can effectively solve the control problems caused by uncertain parameters. In this way, the dynamic performance of the hydraulic system depends heavily on the sliding surface to which the control structure is switched.

Remark 2: On the premise of guaranteeing stability (i.e. $\eta_s > D$), the ability of fast convergence for the system should be concerned. Nevertheless, when the system error is large with notable disturbances, it is natural to set the proportional gain k_s with a large value and vice versa. Hence, it is necessary to use the adjustable control gain instead of a fixed value so that the target system can avoid unexpected chattering problem and stabilize quickly.

In this section, the fuzzy logic methodology is proposed to modulate the proportional gain k_s for the approaching control term. The proposed control strategy adopts a general two-input-one-output fuzzy system as the self-tuning mechanism, whose inputs are related to the sliding surface s and its

derivative of time $\dot{s}$. Then, the fuzzy logic rules for adjusting the proportional control gain are made for the following two cases: (a) If $s\dot{s} > 0$, the state trajectories have a tendency to deviate from the sliding surface. In this case, when the sliding variable is far from the sliding surface or the approaching speed is fast, the proportional gain k_s ought to be correspondingly enlarged to compel the sliding variable to return to the sliding surface as quickly as possible. (b) If $s\dot{s} \leq 0$, the state trajectories have a tendency to move towards the sliding surface. In this case, when the sliding variable is nearly on the sliding surface or the approaching speed is very low, k_s should be very small to ensure that the position error converges to a minimum so as to reduce chattering.

Based on the above considerations, the fuzzy logic system is developed by adopting the Mamdani inference method to describe the fuzzy conditional statements. The fuzzy input variables s and $\dot{s}$ are both scaled and decomposed into five trigonometry/trapezoidal membership functions. The inputs are expressed as NB (Negative Big), NS (Negative Small), ZO (Zero), PS (Positive Small), and PB (Positive Big), and they are normalized to the interval $[-1, 1]$ as depicted in Fig. 3. Besides, as is shown in Fig. 4, the output singleton k_s is labeled by linguistic values ZO (Zero), VS (Very Small), MS (Medium Small), MB (Medium Big) and VB (Very Big), which are normalized to the interval [0, 1]. Each combination of input variable values and corresponding input membership functions activates one approaching control action based on the fuzzy IF-THEN rules. In this case, these fuzzy rules are designed as

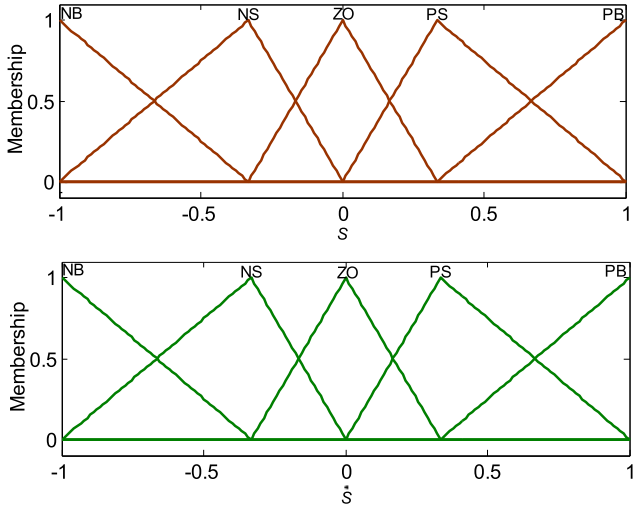

FIGURE 3. The normalized input membership functions for s and $\dot{s}$.

$R^{(j)}$: IF s is F_s^j and $\dot{s}$ is $F_{\dot{s}}^j$, THEN k_s is B^j. where F_s^j and $F_{\dot{s}}^j$ are labels of the s and $\dot{s}$, respectively, and B^j is the corresponding label of output fuzzy subject. Through trial and error, the linguistic fuzzy rules mapping the input to the output are designed in Tab 1.

Then, the fuzzy proportional gain can be obtained by using the singleton fuzzification, product inference engine and the

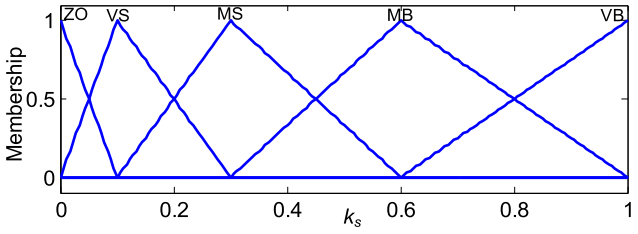

FIGURE 4. The normalized output membership functions for k_s.

TABLE 1. The fuzzy control rules for the proportional gain k_s.

$s/\dot{s}$	NB	NS	ZO	PS	PB
NB	VB	VB	ZO	VS	VS
NS	VB	MB	ZO	VS	VS
ZO	MB	MS	ZO	MS	MS
PS	MS	MS	MS	MB	VB
PB	VB	VS	VS	MB	VB

center average defuzzification as [34]

$$k_{fs} = \frac{\sum_{j=1}^{m} r_j w_{F_s^j}(s)\, w_{F_{\dot{s}}^j}(\dot{s})}{\sum_{j=1}^{m} w_{F_s^j}(s)\, w_{F_{\dot{s}}^j}(\dot{s})} \tag{22}$$

where, m is the number of fuzzy rules, r_j denotes a crisp value at which the output membership function w_{B^j} reaches its maximum value, $w_{F_s^j}, w_{F_{\dot{s}}^j}$ represent the membership function of the linguistic variable s and $\dot{s}$, respectively.

Furthermore, a saturation function is used to replace the sign function, and the approaching term (15) is expressed by

$$u_{fap} = k_{fs}s + \eta_s sat(s) \tag{23}$$

Here, k_{fs} denotes the proportional gain adjusted by a fuzzy logic inference mechanism, and $sat(s)$ represents a saturation function defined as

$$sat\left(\frac{s}{\sigma}\right) = \begin{cases} sgn(s), & if \ \ |s| > \sigma \\ \dfrac{s}{\sigma}, & if \ \ |s| \leq \sigma \end{cases} \tag{24}$$

where $\sigma > 0$ is the thickness of the boundary layer.

Finally, substituting (22) and (23) in (16), the system input will be modified as

$$u = \hat{\phi}_2 x_2 + \hat{\phi}_3 x_3 + \hat{\phi}_1 \left(c_1 e_2 + c_2 e_3 + \ddot{\theta}_d\right) + k_{fs}s + \eta_s sat(s) \tag{25}$$

Reviewing the entire deriving process, the overall block diagram of the proposed controller can be clearly illustrated in Fig. 5.

IV. EXPERIMENTS AND RESULTS

The goal of this paper is to let the actuator track any smooth angle trajectory as closely as possible. Hence, a test platform is built for the position tracking experiments of the valve-controlled hydraulic system, which is addressed in this section.

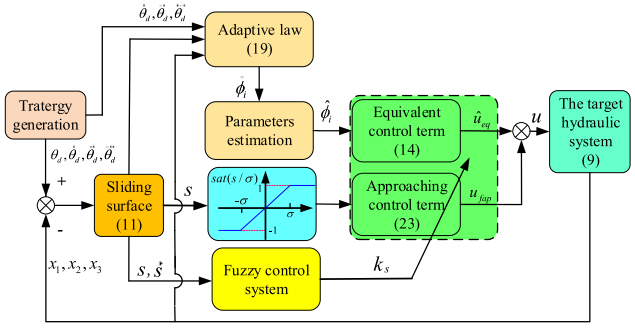

FIGURE 5. The overall block diagram of the AFSMC strategy.

A. EXPERIMENTAL SETUP CONFIGURATION

The real-time control platform of the valve-controlled hydraulic servo system is shown in Fig. 6, which is mainly composed of a real-time control system, a circular hydraulic actuator, an angle sensor with high measurement accuracy providing continuous position signal of the joint, a servo valve (FF101-6, AVIC) utilized to drive the hydraulic actuator, a servo amplifier, a hydraulic supply with $P_s = 4$ Mpa and some terminal boards. In particular, the real-time control system is equipped with two industrial personal computers (IPC-610L, Advantech Inc.), i.e. a host computer and a target computer, and it is set to work in the dual-machine collaborative mode.

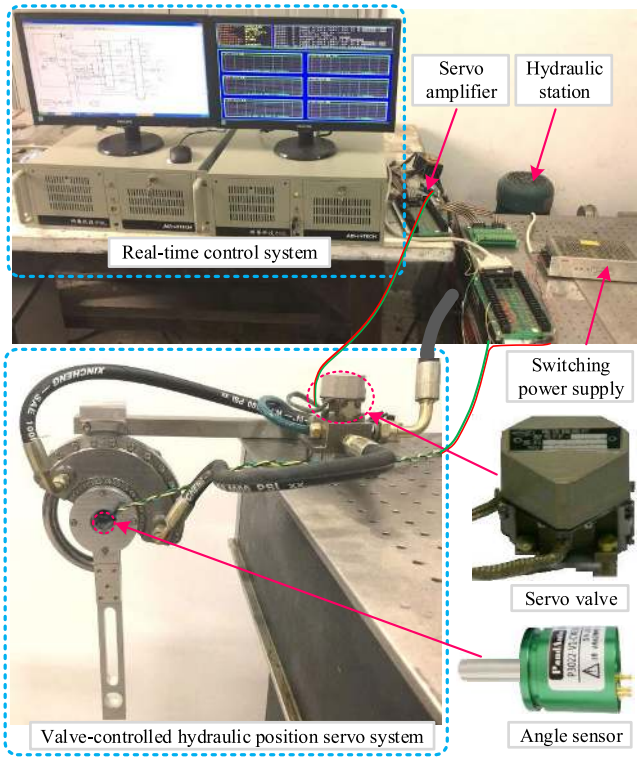

FIGURE 6. Experiment platform of the hydraulic servo system.

Moreover, the host computer is responsible for generating the Simulink control models according to the proposed control strategy and transmits the executable control codes to the target computer through serial communication. The target computer is installed with a real-time-workshop kernel, which is capable of deploying the codes and controlling the hydraulic actuator. In the course of experiment, the target computer acquires the feedback analog signal of the angle sensor through its internal high-precision analog-to-digital (A/D) data acquisition card (PCL-818HD, Advantech Inc.). After that, the measured position signal is filtered in the target computer and compared with the reference signal. The systematic error is processed by the designed controller, and the control command u is sent to the digital-to-analog (D/A) card (PCL-726, Advantech Inc.) of the target computer. Finally, the output analog signal is converted to the corresponding current signal through a power amplifier to control the servo valve. Considering the combined impact of various factors, the sampling periods for the host and target control layers are chosen to be 1ms.

B. TRAJECTORY TRACKING EXPERIMENTS AND RESULTS

Values of the system parameters used in the experiment are shown in Table 2. In order to evaluate the position control performance of the valve-controlled circular hydraulic actuator, the desired tracking signal is selected as $x_d = 20\sin(\pi t/2)$. The parameters of the proposed AFSMC algorithm were selected as $c_1 = 38000$, $c_2 = 600$, $k_s = 3 \times 10^{-5}$, $\eta_s = 0.01$, $\gamma_1 = 1 \times 10^{-17}$, $\gamma_2 = 3 \times 10^{-8}$, and $\gamma_3 = 1 \times 10^{-8}$. Besides, the initial states of the target system are given by $x_1(0) = x_2(0) = x_3(0) = 0$, and the time-varying generalized parameters are preset as in Table 3.

TABLE 2. Main parameters of the hydraulic servo system.

Physical parameters	Values
System oil supply pressure, P_s	$4 \times 10^6\ Pa$
Oil effective bulk modulus, β_e	$7.45 \times 10^8\ Pa$
Viscous damping coefficient, B_t	$600\ N/(m/s)$
Inertia moment of the piston rod and payload, J_l	$0.06\ kg \cdot m^2$
Effective ram area of the rod chamber, A_1	$0.24 \times 10^{-3}\ m^2$
Effective ram area of the rodless chamber, A_2	$0.49 \times 10^{-3}\ m^2$
Total chamber volume, V_{10}	$20.93 \times 10^{-6}\ m^3$
Total chamber volume, V_{20}	$69.69 \times 10^{-6}\ m^3$
Linear coefficient, K_v	$1.26 \times 10^{-4}\ m/V$
Flow gain coefficient, K_{q0}	$0.342\ m^2/s$
Flow pressure coefficient, K_{c0}	$4.8 \times 10^{-12}\ m^3/(Pa \cdot s)$

TABLE 3. Numerical range of generalized parameters.

Parameters	Initial values	Lower limit values	Upper limit values
ϕ_1	1.1×10^{-6}	1.1×10^{-7}	1.1×10^{-5}
ϕ_2	3.7×10^{-1}	3.7×10^{-2}	3.7×10^{0}
ϕ_3	9.6×10^{-3}	9.6×10^{-4}	9.6×10^{-2}

To apply our proposed controller, the model parameters of target system are set to zero, and the results of trajectory tracking experiments are shown in Fig. 7 and Fig. 8. Here, Fig. 7 shows the real-time trajectory tracking and the

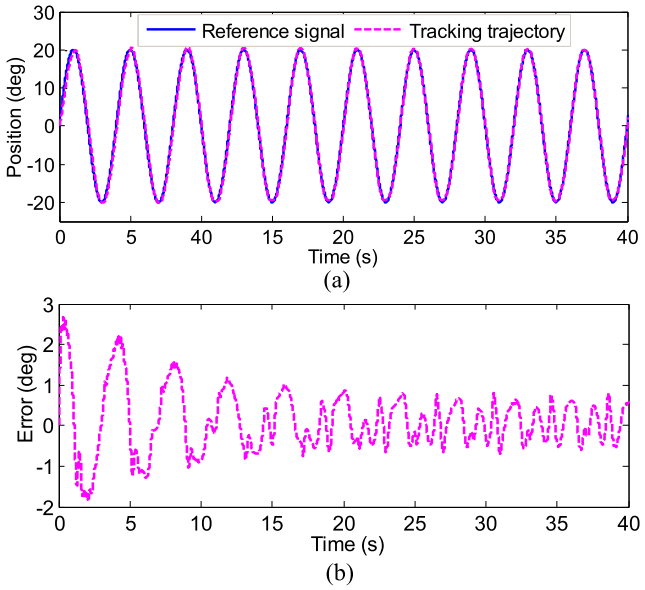

FIGURE 7. Trajectory tracking results of the proposed controller. (a) Comparisons between the desired trajectory and the actual trajectory; (b) The position tracking error.

corresponding tracking errors of the actuator, from which we can see that the actuator can move in real time according with the reference position signal. In particular, the measured output and reference output are very similar after 20 seconds, indicating excellent position tracking performance of the proposed controller. The process of parameter estimations and self-adjustment of proportional gain are illustrated in Fig. 8. It can be seen that the uncertain parameters ϕ_1, ϕ_2, and ϕ_3 are asymptotically convergent, meanwhile, the proportional gain k_s has the self-tuning and time-varying characteristics.

In addition, the PID controller and a conventional exponential approaching SMC controller are implemented to validate the advantages of the proposed control scheme. Through trial and error, the parameters of the PID controller are selected as $k_p = 1.8$, $k_i = 0.16$, and $k_d = 0.09$. The parameters of the exponential approaching SMC controller are the same as the AFSMC except that the system parameter variations and self-adjustable proportional gain are not considered for SMC. For comparison, three tracking experiments of the actiator using PID, SMC and AFSMC are conducted in the following two cases.

Case 1: When the payload is zero, the tracking performance using three different controllers are shown in Fig. 9. In Fig. 9(a), the position tracking curves are consistent and their corresponding tracking errors are bounded and periodically stable. All controllers can let the actuator follow the reference trajectory and have good dynamic response performance. As depicted in Fig. 9b, the tracking errors of PID controller fluctuates in the range of $-1.2° \sim 1.4°$, while the tracking errors of SMC and ASMC are well contained within the range of $\pm 1°$ and $\pm 0.8°$, respectively. Therefore, the tracking performance is the best with the proposed AFSMC controller which considers the parameters estimation and variable gain k_s.

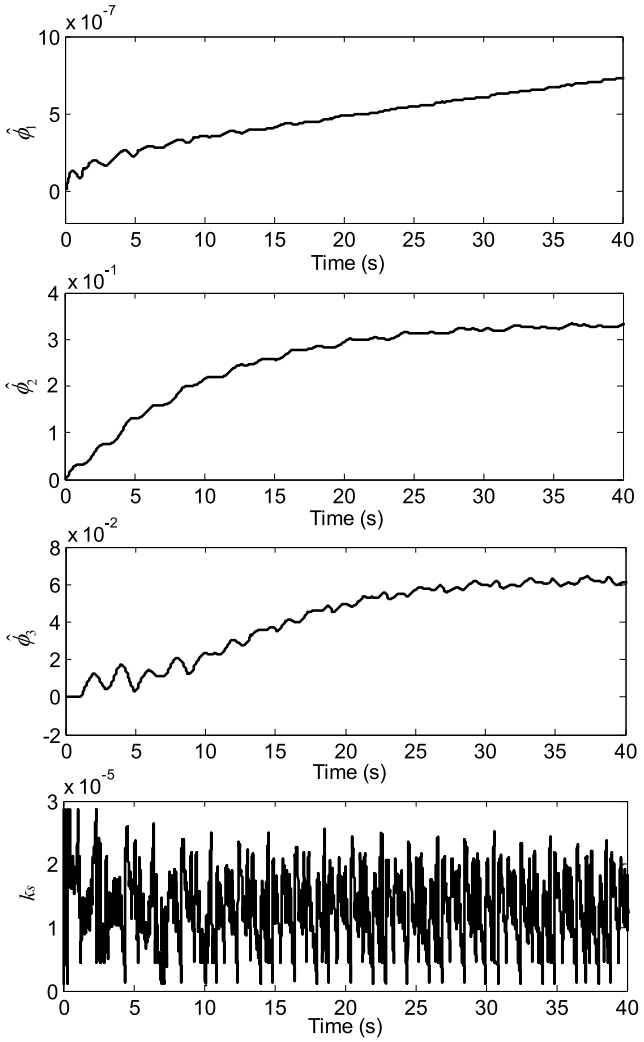

FIGURE 8. The process of parameter estimations.

Case 2: To further evaluate the robustness of the designed controller, a payload of 10Kg is added to the actuator. In Fig.10(a), the position tracking curve of the PID controller has burrs near its peak amplitudes, whereas the other two controllers remain almost unchanged. Accordingly in Fig.10(b), the tracking error of PID controller significantly increases from $-1.2°$ to $-1.4°$. As seen, in case that the payload of the system increases, the performance of the PID controller will deteriorate and the tracking error will also remarkably raise. Besides, the experimental phenomenon also denotes that both of the SMC controller and the proposed control scheme have more capability to suppress disturbance. It indicates that the PID controller is very sensitive to external disturbances, while the performance of the other two controllers is not so obvious.

In general, since the parameters estimation and variable gain k_s were considered to reduce the chattering problem, the proposed AFSMC exhibits better position control accuracy than conventional exponential approaching SMC and PID controller.

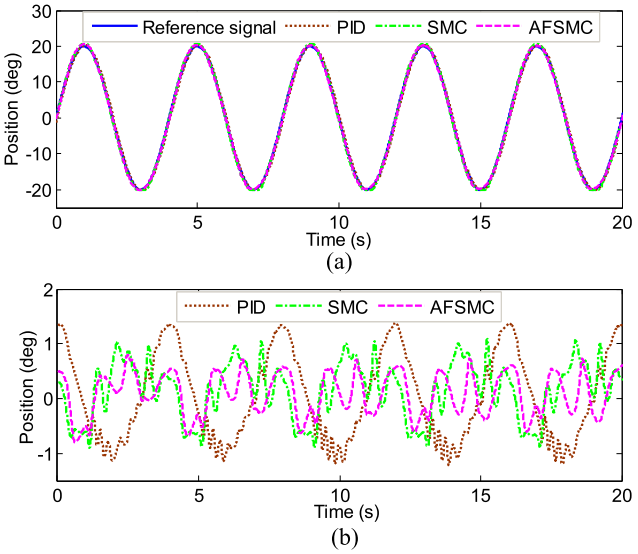

FIGURE 9. Performance comparison of different control strategies for the actuator under no-load. (a) Comparisons between the desired trajectory and the actual trajectory; (b) Comparison of position tracking errors.

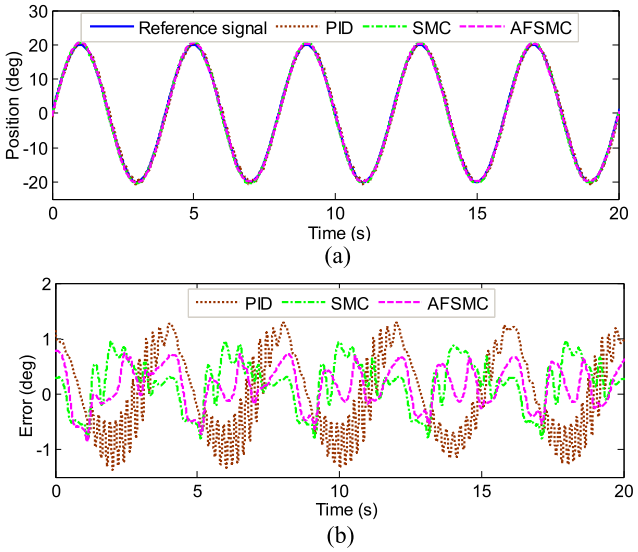

FIGURE 10. Performance comparison of different control strategies for the actuator under 10Kg payload. (a) Comparisons between the desired trajectory and the actual trajectory; (b) Comparison of position tracking errors.

V. CONCLUSION

In this study, an adaptive sliding mode control that incorporates a fuzzy tuning technique for trajectory tracking of a circular hydraulic actuator has been proposed. Firstly, the major mechanical structure design of the actuator was briefly described. And then, the dynamic characteristics of valve-controlled hydraulic position system were analyzed and its state space form was established. To overcome the influence of parameter uncertainty, an adaptive estimation law was derived via the Lyapunov stability theory and the discontinuous projection algorithm was also introduced. After that, a fuzzy controller was proposed to modulate the proportional gain k_s of approaching control term to restrain undesirable chattering and reduce the time required to reach the sliding surface. Finally, a real-time control platform of the valve-controlled hydraulic system was built, and the position tracking experiments of the actuator were carried out with different control algorithms. The experimental results demonstrated that the designed controller has higher position control accuracy and stronger robustness compared with the conventional PID and exponential approaching SMC methods.

REFERENCES

[1] Q. Guo, Y. Zhang, B. G. Celler, and S. W. Su, "Backstepping control of electro-hydraulic system based on extended-state-observer with plant dynamics largely unknown," *IEEE Trans. Ind. Electron.*, vol. 63, no. 11, pp. 6909–6920, Nov. 2016.

[2] H. Ren and P. Gong, "Adaptive control of hydraulic position servo system using output feedback," *Proc. Inst. Mech. Eng. Part I-J. Syst. Control Eng.*, vol. 231, no. 7, pp. 527–540, Aug. 2017.

[3] C. Sun, J. Fang, J. Wei, and B. Hu, "Nonlinear motion control of a hydraulic press based on an extended disturbance observer," *IEEE Access*, vol. 6, pp. 18502–18510, 2018.

[4] B. Haus, H. Aschemann, and P. Mercorelli, "Tracking control of a piezo-hydraulic actuator using input-output linearization and a cascaded extended Kalman filter structure," *J. Franklin Inst.-Eng. Appl. Math.*, vol. 355, no. 18, pp. 9298–9320, 2018.

[5] K. Guo, J. Wei, J. Fang, R. Feng, and X. Wang, "Position tracking control of electro-hydraulic single-rod actuator based on an extended disturbance observer," *Mechatronics*, vol. 27, pp. 47–56, 2015.

[6] Q. Guo, P. Sun, J.-M. Yin, T. Yu, and D. Jiang, "Parametric adaptive estimation and backstepping control of electro-hydraulic actuator with decayed memory filter," *ISA Trans.*, vol. 62, pp. 202–214, 2016.

[7] P. Mercorelli and N. Werner, "An adaptive resonance regulator design for motion control of intake valves in camless engine systems," *IEEE Trans. Ind. Electron.*, vol. 64, no. 4, pp. 3413–3422, Apr. 2017.

[8] W. Ma, W. Deng, and J. Yao, "Continuous integral robust control of electro-hydraulic systems with modeling uncertainties," *IEEE Access*, vol. 6, pp. 46146–46156, 2018.

[9] J. Yao, W. Deng, and Z. Jiao, "Adaptive control of hydraulic actuators with LuGre model-based friction compensation," *IEEE Trans. Ind. Electron.*, vol. 62, no. 10, pp. 6469–6477, Oct. 2015.

[10] H. Guo, Y. Liu, G. Liu, and H. Li, "Cascade control of a hydraulically driven 6-DOF parallel robot manipulator based on a sliding mode," *Control Eng. Pract.*, vol. 16, no. 9, pp. 1055–1068, 2008.

[11] Y. Lin, Y. Shi, and R. Burton, "Modeling and robust discrete-time sliding-mode control design for a fluid power electrohydraulic actuator (EHA) system," *IEEE/ASME Trans. Mechatronics*, vol. 18, no. 1, pp. 1–10, Feb. 2013.

[12] T. X. Dinh, T. D. Thien, T. H. V. Anh, and K. K. Ahn, "Disturbance observer based finite time trajectory tracking control for a 3 DOF hydraulic manipulator including actuator dynamics," *IEEE Access*, vol. 6, pp. 36798–36809, 2018.

[13] M. Radgolchin and H. Moeenfard, "Development of a multi-level adaptive fuzzy controller for beyond pull-in stabilization of electrostatically actuated microplates," *J. Vib. Control*, vol. 24, no. 5, pp. 860–878, Mar. 2018.

[14] C. Guan and S. Pan, "Adaptive sliding mode control of electro-hydraulic system with nonlinear unknown parameters," *Control Eng. Pract.*, vol. 16, no. 11, pp. 1275–1284, 2008.

[15] A. Mohanty, S. Gayaka, and B. Yao, "An adaptive robust observer for velocity estimation in an electro-hydraulic system," *Int. J. Adapt. Control Signal Process.*, vol. 26, no. 12, pp. 1076–1089, 2012.

[16] G. Palli, S. Strano, and M. Terzo, "Sliding-mode observers for state and disturbance estimation in electro-hydraulic systems," *Control Eng. Pract.*, vol. 74, pp. 58–70, 2018.

[17] D.-T. Tran, H.-V.-A. Truong, and K. K. Ahn, "Adaptive backstepping sliding mode control based RBFNN for a hydraulic manipulator including actuator dynamics," *Appl. Sci.*, vol. 9, no. 6, 2019.

[18] Q. P. Ha, Q. H. Nguyen, D. C. Rye, and H. F. Durrant-Whyte, "Fuzzy sliding-mode controllers with applications," *IEEE Trans. Ind. Electron.*, vol. 48, no. 1, pp. 38–46, Feb. 2001.

[19] W. M. Bessa, M. S. Dutra, and E. Kreuzer, "Sliding mode control with adaptive fuzzy dead-zone compensation of an electro-hydraulic servo-system," *J. Intell. Robot. Syst.*, vol. 58, no. 1, pp. 3–16, Apr. 2010.

[20] N. M. Tri, D. X. Ba, and K. K. Ahn, "A gain-adaptive intelligent nonlinear control for an electrohydraulic rotary actuator," *Int. J. Precis. Eng. Manuf.*, vol. 19, no. 5, pp. 665–673, May 2018.

[21] S. Song, X. Zhang, and Z. Tan, "Rbf neural network based sliding mode control of a lower limb exoskeleton suit," *Strojni ki Vestnik-J. Mech. Eng.*, vol. 60, no. 6, pp. 437–446, 2014.

[22] L. Zhu, Z. Wang, Y. Zhou, and Y. Liu, "Adaptive neural network saturated control for MDF continuous hot pressing hydraulic system with uncertainties," *IEEE Access*, vol. 6, pp. 2266–2273, 2018.

[23] A. Chatterjee, R. Chatterjee, F. Matsuno, and T. Endo, "Augmented stable fuzzy control for flexible robotic arm using LMI approach and neuro-fuzzy state space modeling," *IEEE Trans. Ind. Electron.*, vol. 55, no. 3, pp. 1256–1270, Mar. 2008.

[24] R. Precup, M. Tomescu, and C. Dragos, "Stabilization of Rössler chaotic dynamical system using fuzzy logic control algorithm," *Int. J. Gen. Syst.*, vol. 43, no. 5, pp. 413–433, Jul. 2014.

[25] H. Ho, Y. Wong, and A. Rad, "Adaptive fuzzy sliding mode control with chattering elimination for nonlinear SISO systems," *Simul. Model. Pract. Theory*, vol. 17, no. 7, pp. 1199–1210, 2009.

[26] R.-J. Wai and K.-H. Su, "Adaptive enhanced fuzzy sliding-mode control for electrical servo drive," *IEEE Trans. Ind. Electron.*, vol. 53, no. 2, pp. 569–580, Apr. 2006.

[27] S. Wang, R. Burton, and S. Habibi, "Sliding mode controller and filter applied to an electrohydraulic actuator system," *J. Dyn. Syst. Meas. Control-Trans. ASME*, vol. 133, no. 2, Mar. 2011.

[28] W. Kim, D. Won, D. Shin, and C. C. Chung, "Output feedback nonlinear control for electro-hydraulic systems," *Mechatronics*, vol. 22, no. 6, pp. 766–777, 2012.

[29] H.-M. Chen, J.-C. Renn, and J.-P. Su, "Sliding mode control with varying boundary layers for an electro-hydraulic position servo system," *Int. J. Adv. Manuf. Technol.*, vol. 26, no. 1, pp. 117–123, Jul. 2005.

[30] Z. Has, M. F. Rahmat, A. R. Husain, K. Ishaque, R. Ghazali, M. N. Ahmad, Y. M. Sam, and S. M. Rozali, "Robust position tracking control of an electro-hydraulic actuator in the presence of friction and internal leakage," *Arabian J. Sci. Eng.*, vol. 39, no. 4, pp. 2965–2978, Apr. 2014.

[31] M. Jerouane, N. Sepehri, and F. Lamnabhi-Lagarrigue, "Dynamic analysis of variable structure force control of hydraulic actuators via the reaching law approach," *Int. J. Control*, vol. 77, no. 14, pp. 1260–1268, 2004.

[32] C. J. Fallaha, M. Saad, H. Y. Kanaan, and K. Al-Haddad, "Sliding-mode robot control with exponential reaching law," *IEEE Trans. Ind. Electron.*, vol. 58, no. 2, pp. 600–610, Feb. 2011.

[33] L. Ren, S. Xie, Y. Zhang, J. Peng, and L. Zhang, "Chattering analysis for discrete sliding mode control of distributed control systems," *J. Syst. Eng. Electron.*, vol. 27, no. 5, pp. 1096–1107, Oct. 2016.

[34] M. B. Nazir and S. Wang, "Optimized fuzzy sliding mode control to enhance chattering reduction for nonlinear electro-hydraulic servo system," *Int. J. Fuzzy Syst.*, vol. 12, no. 4, pp. 291–299, 2010.

[35] T. H. Ho and K. K. Ahn, "Speed control of a hydraulic pressure coupling drive using an adaptive fuzzy sliding-mode control," *IEEE/ASME Trans. Mechatronics*, vol. 17, no. 5, pp. 976–986, Oct. 2012.

[36] O. Cerman and P. Husek, "Adaptive fuzzy sliding mode control for electro-hydraulic servo mechanism," *Expert Syst. Appl.*, vol. 39, no. 11, pp. 10269–10277, 2012.

[37] M. Yang, Q. Zhu, R. Xi, X. Wang, and Y. Han, "Design of the power-assisted hip exoskeleton robot with hydraulic servo rotary drive," in *Proc. 23rd Int. Conf. Mechatronics Mach. Vis. Pract. (M2VIP)*, Nov. 2016, pp. 1–5.

[38] Y. Ye, C.-B. Yin, Y. Gong, and J.-J. Zhou, "Position control of nonlinear hydraulic system using an improved PSO based PID controller," *Mech. Syst. Signal Proc.*, vol. 83, pp. 241–259, 2017.

[39] Y. Tang, Z. Zhu, G. Shen, and W. Zhang, "Real time acceleration tracking of electro-hydraulic shake tables combining inverse compensation technique and neural-based adaptive controller," *IEEE Access*, vol. 5, pp. 23681–23694, 2017.

MINGXING YANG was born in Shandong, China, in 1986. He received the M.S. degree in mechanical design and theory from the Shandong University of Technology, Zibo, China, in 2014. He is currently pursuing the Ph.D. degree with the School of Mechanical Engineering, Southeast University, Nanjing, China.

His major research interests include servo control of mechatronic systems, robust adaptive control, and powered exoskeleton robots.

KAIWEI MA received the M.S. degree in mechanical and automotive engineering from the Xiamen University of Technology, Xiamen, China, in 2016. He is currently pursuing the Ph.D. degree with the School of Mechanical Engineering, Southeast University, Nanjing, China.

His recent research projects include robotic belt grinding systems, special reducer for robot, and machine vision for mechatronics systems. His research interests include intelligent control, image processing, and complex surface machining.

YUNDE SHI received the B.S. degree from Shanghai Jiao Tong University, Shanghai, China, in 2008, and the M.S. and Ph.D. degrees from Columbia University, New York, NY, USA, in 2009 and 2013, respectively, all in mechanical engineering.

He was a Senior Engineer with the Servo Format Group, Seagate Technology, Shakopee, MN, USA, from January 2013 to January 2016. He is currently an Associate Professor with Southeast University, Nanjing, China. His research interests include the fields of learning control, unmanned autonomous systems, and rehabilitation robots.

XINGSONG WANG received the B.S. and M.S. degrees from Zhejiang University, Hangzhou, China, in 1988 and 1991, respectively, and the Ph.D. degree from Southeast University, Nanjing, China, in 2000, all in mechanical engineering.

He was a Visiting Scientist with the School of Mechanical Engineering, Concordia University, Montreal, QC, Canada, from June 2000 to December 2000 and September 2001 to March 2002, and the School of Mechanical Engineering, Purdue University, West Lafayette, IN, USA, from September 2007 to March 2008. He is currently a Full Professor with the School of Mechanical Engineering and the Head of the Department of Mechatronics, Southeast University. His current research interests include control theory with application in precision CNC machine tools, advanced mechatronics with applications in biomedical engineering, and intelligent manufacturing.